

## 23ME-00610, a genetically informed, first-in-class antibody targeting CD200R1 to enhance antitumor T cell function

Jill Fenaux<sup>a#</sup>, Xin Fang<sup>b#</sup>, Yao-ming Huang<sup>c</sup>, Cristina Melero<sup>c</sup>, Caroline Bonnans<sup>d</sup>, Earth Light Lowe<sup>d</sup>, Tiziana Palumbo<sup>d</sup>, Cecilia Lay<sup>a</sup>, Zuoan Yi<sup>a</sup>, Aileen Zhou<sup>a</sup>, Mauro Poggio<sup>a</sup>, Wei-Jen Chung<sup>b</sup>, Sophia R. Majeed<sup>e</sup>, Dylan Glatt<sup>f</sup>, Alice Chen<sup>a</sup>, Maike Schmidt<sup>g</sup>, and Clarissa C. Lee<sup>a</sup>

<sup>a</sup>Immuno-Oncology, 23andMe, South San Francisco, CA, USA; <sup>b</sup>Computational Biology, 23andMe, South San Francisco, CA, USA; <sup>c</sup>Antibody and Protein Engineering, 23andMe, South San Francisco, CA, USA; <sup>d</sup>In Vivo Pharmacology, 23andMe, South San Francisco, CA, USA; <sup>e</sup>Clinical Science, 23andMe, South San Francisco, CA, USA; <sup>f</sup>Clinical Pharmacology, 23andMe, South San Francisco, CA, USA; <sup>g</sup>Biomarker Translation, 23andMe, South San Francisco, CA, USA

### ABSTRACT

Immune checkpoint inhibition (ICI) has revolutionized cancer treatment; however, only a subset of patients benefit long term. Therefore, methods for identification of novel checkpoint targets and development of therapeutic interventions against them remain a critical challenge. Analysis of human genetics has the potential to inform more successful drug target discovery. We used genome-wide association studies of the 23andMe genetic and health survey database to identify an immuno-oncology signature in which genetic variants are associated with opposing effects on risk for cancer and immune diseases. This signature identified multiple pathway genes mapping to the immune checkpoint comprising CD200, its receptor CD200R1, and the downstream adapter protein DOK2. We confirmed that CD200R1 is elevated on tumor-infiltrating immune cells isolated from cancer patients compared to the matching peripheral blood mononuclear cells. We developed a humanized, effectorless IgG1 antibody (23ME-00610) that bound human CD200R1 with high affinity ( $K_D < 0.1$  nM), blocked CD200 binding, and inhibited recruitment of DOK2. 23ME-00610 induced T-cell cytokine production and enhanced T cell-mediated tumor cell killing in vitro. Blockade of the CD200:CD200R1 immune checkpoint inhibited tumor growth and engaged immune activation pathways in an S91 tumor cell model of melanoma in mice.

### ARTICLE HISTORY

Received 17 January 2023  
Revised 1 May 2023  
Accepted 22 May 2023

### KEYWORDS

23ME-00610; cancer immunotherapy; CD200; CD200R1; immune checkpoint

## Introduction

Antibodies targeting immune checkpoints, such as those mediated by cytotoxic T-lymphocyte-associated protein 4 (CTLA-4) and programmed cell death protein-1 (PD-1), provide strong antitumor activity and result in improved overall survival across numerous solid and hematologic cancers<sup>1</sup>. However, many patients fail to respond to or ultimately relapse after checkpoint inhibitor treatment. One component of nonresponse (or relapse) may be engagement of other, compensatory immune checkpoints by tumor cells that allow them to circumvent inhibition of established checkpoints<sup>1</sup>. Therefore, identification and modulation of additional immune checkpoints may provide clinical benefit for non-responsive or resistant patients.


CD200R1 is an immune inhibitory receptor mainly expressed on CD4<sup>+</sup> and CD8<sup>+</sup> T cells and myeloid cells<sup>2,3</sup>. While CD200R1 expression is predominantly limited to immune cells, its ligand CD200 is expressed in a variety of normal and cancer cells<sup>4</sup>. Binding of CD200 to CD200R1 results in phosphorylation of the intracellular tail of CD200R1, recruitment of DOK2 and RasGAP, and subsequent inhibition of ERK and Akt signaling pathways<sup>5-7</sup>. In vivo and in vitro studies have revealed that signaling through the

CD200:CD200R1 pathway downregulates the production of proinflammatory cytokines by T cells and/or activated myeloid cells<sup>7,8</sup>. Moreover, activation of CD200:CD200R1 signaling in vivo tempers the immune response to infectious agents and is protective against autoimmune diseases and lung inflammation in asthma models<sup>4,9</sup>.

We hypothesized that identifying genetic variants with pleiotropic, opposing effects in cancer and immune diseases could be used to identify immuno-oncology (I/O) targets involved in regulating the antitumor immune response. Using this approach, we identified CD200R1, CD200, and DOK2 as potential I/O targets. We found that CD200R1 is highly correlated with T cell markers across cancer types in The Cancer Genome Atlas (TCGA) and observed that CD200R1 was most prevalently expressed on exhausted T cells in patients who have received ICI therapy. With the aim of blocking CD200R1 on tumor-infiltrating lymphocytes (TILs) to relieve immunosuppression, we developed a first-in-class, anti-CD200R1 monoclonal antibody (mAb), 23ME-00610. 23ME-00610 bound human CD200R1 with high affinity ( $K_D < 0.1$  nM) and rescued T cells from the direct immunosuppressive effects of CD200. Blocking the CD200:CD200R1 immune checkpoint reduced tumor cell growth both in vitro

**CONTACT** Clarissa C. Lee  [clarissal@23andme.com](mailto:clarissal@23andme.com)  23andMe, 349 Oyster Point Blvd, South San Francisco, CA 94080, USA

#coauthors.

 Supplemental data for this article can be accessed online at <https://doi.org/10.1080/2162402X.2023.2217737>.

© 2023 23andMe. Published with license by Taylor & Francis Group, LLC.

This is an Open Access article distributed under the terms of the Creative Commons Attribution-NonCommercial License (<http://creativecommons.org/licenses/by-nc/4.0/>), which permits unrestricted non-commercial use, distribution, and reproduction in any medium, provided the original work is properly cited. The terms on which this article has been published allow the posting of the Accepted Manuscript in a repository by the author(s) or with their consent.

and in vivo, supporting the hypothesis that blocking the CD200R1 immune checkpoint has the potential to prevent or reverse immune-cell tolerance in the tumor microenvironment (TME).

## Methods

Brief summaries of methods are provided below; for detailed descriptions of each method, refer to the Supplemental Methods.

Consented research participants were genotyped using an SNP microarray, and genotype imputation was performed using standard methodologies. GWAS analysis used genotype and phenotype data (collected via survey) from unrelated individuals. GWAS hits were annotated using > 60 published eQTL and QTL datasets. To identify GWAS signals ( $p$  value <  $5e-8$ ) that potentially share a common causal variant across phenotypes, we clustered GWAS signals using linkage disequilibrium between the index SNPs with a cutoff of  $r^2 \geq 0.8$ . We then searched for CTLA4-like pleiotropic signatures among GWAS signal clusters that have opposite direction of effect in cancer and immune phenotypes. Public gene expression data from TCGA were filtered and analyzed using custom scripts in R. Single-cell RNA-seq melanoma datasets, including transcript per million (TPM) values, cell cluster annotation, t-Distributed Stochastic Neighbor Embedding (TSNE) coordinates, and clinical metadata were downloaded from GEO: GSE120575.

In-house RNA-seq analysis was performed on total RNA isolated from homogenized mouse tissue. The library was prepared using an Illumina Stranded mRNA Prep Ligation kit and sequenced on an Illumina NovaSeq 1.5 v platform.

Recombinant, His- or Fc-tagged proteins were expressed in mammalian cells and purified by sequential affinity purification and size-exclusion chromatography. Binding affinity of 23ME-00610 for recombinant CD200R1 isoforms was performed using a BIACORE 8K SPR instrument at 37 °C.

Expression of CD200 or CD200R1 on TILs or cell lines was evaluated using flow cytometry. Displacement of CD200 from U937 cells expressing CD200R1 by 23ME-00610 was evaluated by flow cytometry. Secretion of cytokines from immune cells was evaluated by commercial ELISA or Luminex. Real-time imaging of COV644-GFP cell growth co-cultured with human PBMCs in the presence of 23ME-00610 or isotype control was performed using an IncuCyte imaging system. To quantify the tumor cell killing potency of 23ME-00610, the area under the curve (AUC) of the killing phase was converted to COV644 tumor cell killing relative to isotype control using the following equation:

$$\% \text{ PBMC-mediated tumor cell killing (conc)} = \frac{\text{Isotype AUC, GFP} - \text{23ME-00610 AUC, GFP (conc)}}{\text{Isotype AUC, GFP}}$$

To evaluate the antitumor efficacy of anti-CD200 (Fc-silent OX90), 6- to 8-week old, female DBA/2 mice were injected subcutaneously (SC) with Cloudman S91 melanoma cells in 50% Matrigel. Expression of CD200 on S91 tumor cells was confirmed by flow cytometry. Once implanted tumors reached 80–100 mm<sup>3</sup> volume, mice were randomized into 2 groups of 15 mice and treated by IP injection twice per week with either isotype control or OX90 (20 mg/kg). Tumor volume and body weight were measured twice per week. All in vivo experiments were conducted with the approval of the Institutional Animal Care and Use Committee (IACUC) of 23andMe.

## Results

### **Identification of CD200R1 as a novel immuno-oncology target differentially expressed on tumor-infiltrating lymphocytes and peripheral blood mononuclear cells**

The 23andMe genetic and health survey database was used to conduct genome-wide association studies (GWAS) across multiple phenotypes to identify genetic variants with pleiotropic, opposing effects in cancer and immune diseases. We hypothesized that such variants could be used to identify I/O targets that are involved in regulating the antitumor immune response<sup>10</sup>. Notably, a variant (rs3087243) mapping to CTLA4 was associated with opposing direction of effects (risk vs. benefit) on autoimmune and inflammatory diseases and cancer, supporting this approach (Figure 1A).

A similar pleiotropic I/O signature was observed for three genomic loci in the GWAS analysis tagged by the following three SNPs: rs140763487, rs1131199, rs34215892 (Supplemental Table S1). These variants mapped to genes encoding CD200R1, its sole ligand CD200, and the downstream signaling protein DOK2, respectively (Figure 1B, C). This analysis suggests that, similar to the established I/O target CTLA4, blockade of the CD200:CD200R1 checkpoint axis has the potential to activate an anti-tumor immune response.

We next evaluated the distribution and prevalence of CD200R1 among immune-cell subsets within human tumors. Analysis of 9571 tumor samples from 32 tumor types in the TCGA database revealed a positive correlation between the RNA expression of *CD200R1* and immune-cell markers representative of T cells and myeloid cells. Correlation ( $\rho > 0.5$ ) between *CD200R1* and *CD45* was observed in 30 of 32 (30/32) tumor types examined (Supplemental Figure S1). Similarly, correlation ( $\rho > 0.5$ ) was observed between *CD200R1* and *CD8A*, *CD4*, and *CD11B* in 25/32, 27/32, and 21/32 tumor types, respectively. Representative correlation data for patients with renal clear cell carcinoma are shown in Figure 2A due to high immune infiltration in this cancer type.

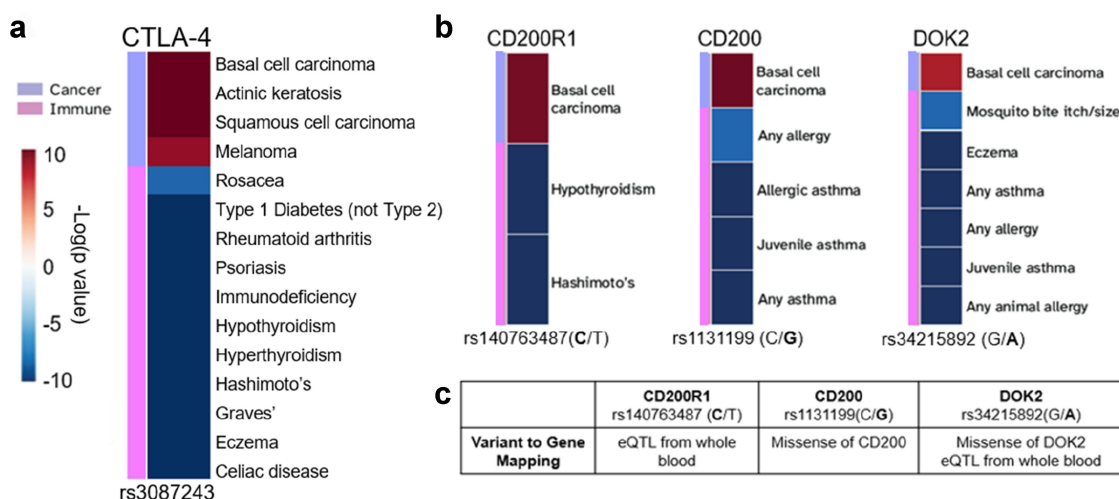


**Figure 1.** Identification of the immune checkpoint protein CD200R1 as a novel immuno-oncology target. GWAS analysis was performed using genetic and phenotypic information in the 23andMe database. Phenotypic data are derived from medical surveys that capture the cancer- and immune-related diseases of participants. a) Heatmap corresponding to the  $-\log(p)$  value of the GWAS (capped at -10 and 10 for visualization) multiplied by the sign of the effect (-1 or 1 indicated in blue or red) for a variant rs3087243(A/G) mapping to CTLA4 via eQTL, showing opposing effects on cancer (violet) and immune diseases (pink), thereby defining an I/O genetic signature. The color (blue to red) corresponds with the direction of the effect. b) Heatmaps for the 3 variants (rs140763487, rs1131199, rs34215892) corresponding to CD200R1, CD200, and DOK2, respectively. Test alleles for which the direction of effect is specified are shown in bold. c) Evidence supporting variant to gene mapping.

To determine CD200R1 expression on immune-cell subsets, especially in the context of prior immune checkpoint therapy, we analyzed single-cell RNA-seq data from 48 tumor samples isolated from patients with melanoma previously treated with anti-PD-1, anti-CTLA-4, or combination therapy<sup>11</sup>. *CD200R1* was highly represented among exhausted T cells and lymphocytes in all samples (Figure 2B, C). Furthermore, while *CD200R1* expression is observed in both responders and non-responders to immune checkpoint inhibitor therapy, cell-type prevalence differed between these two groups. In particular, exhausted T cells were enriched in nonresponders, which may contribute to the overall higher expression of *CD200R1* in this population (Supplemental Figure S2).

To determine if CD200R1 is expressed differentially in the TME compared to the periphery, we compared CD200R1 protein expression on immune cells from dissociated tumor tissue with that of matched peripheral blood mononuclear cells (PBMCs) by flow cytometry. We observed a significant increase in CD200R1 protein expression on tumor-infiltrating CD4<sup>+</sup> and CD8<sup>+</sup> T cells and B cells, relative to the periphery, in samples from five different cancer types (Figure 2D).

Collectively, these expression analyses confirm that CD200R1 is expressed in TILs across a wide variety of human cancer types, suggesting that CD200R1 may play a role in the immunosuppressive TME in humans.

### Characterization of 23ME-00610, an anti-CD200R1 monoclonal antibody

To study the potential of CD200:CD200R1 blockade as a method to relieve tumor-cell immunosuppression in humans, we generated a mAb (23ME-00610) against the extracellular domain of human CD200R1. 23ME-00610 is a humanized IgG1 mAb that is aglycosylated due to an

engineered asparagine to glycine mutation (N297G), which attenuates binding to Fc $\gamma$  receptors and thereby impairs Fc-mediated effector function (Supplemental Figure S3).

We sought to characterize the binding parameters of 23ME-00610 for each functional form of CD200R1 expressed in humans (Supplemental Table S2 and Table S3). When evaluated by surface plasmon resonance (SPR), 23ME-00610 bound purified, recombinant extracellular domains of all functionally relevant isoforms and haplotypes of human CD200R1 with  $K_D$  values in the picomolar to low nanomolar range (Supplemental Table S4) (Figure 3A). To study binding in a more physiological context, we evaluated the binding of 23ME-00610 to CD200R1 expressed on the surface of primary human immune cells. 23ME-00610 bound cell-surface CD200R1 on human T cells from 3 individual donors with a mean half-maximal effective concentration ( $EC_{50}$ )  $\pm$  standard deviation (SD) of  $0.34 \pm 0.03$  nM. Representative data from one donor corresponded to an  $EC_{50}$  of 0.27 nM and 0.32 nM for CD4<sup>+</sup> and CD8<sup>+</sup> T cells, respectively (Figure 3B). Similarly, 23ME-00610 bound cell-surface human CD200R1 expressed on primary human monocyte-derived dendritic cells (MoDCs) with an  $EC_{50}$  of  $0.55 \pm 0.07$  nM ( $n = 3$  donors) (Supplemental Figure S4).

We next evaluated whether 23ME-00610 could block the binding of CD200 to CD200R1. Using an enzyme-linked immunosorbent assay (ELISA), 23ME-00610 pre-incubated with soluble CD200R1 blocked the binding of the receptor to plate-immobilized, Fc-tagged CD200 with a half-maximal inhibition constant ( $IC_{50}$ ) of 0.34 nM. (Supplemental Figure S5). We sought to evaluate 23ME-00610 in a system more relevant to the TME, where CD200 on tumor cells are likely to be bound to CD200R1 on TILs. When monocytic U937 cells exogenously expressing CD200R1 were pre-incubated with concentrations of biotinylated CD200 ranging from 2 to 800 nM, 23ME-00610

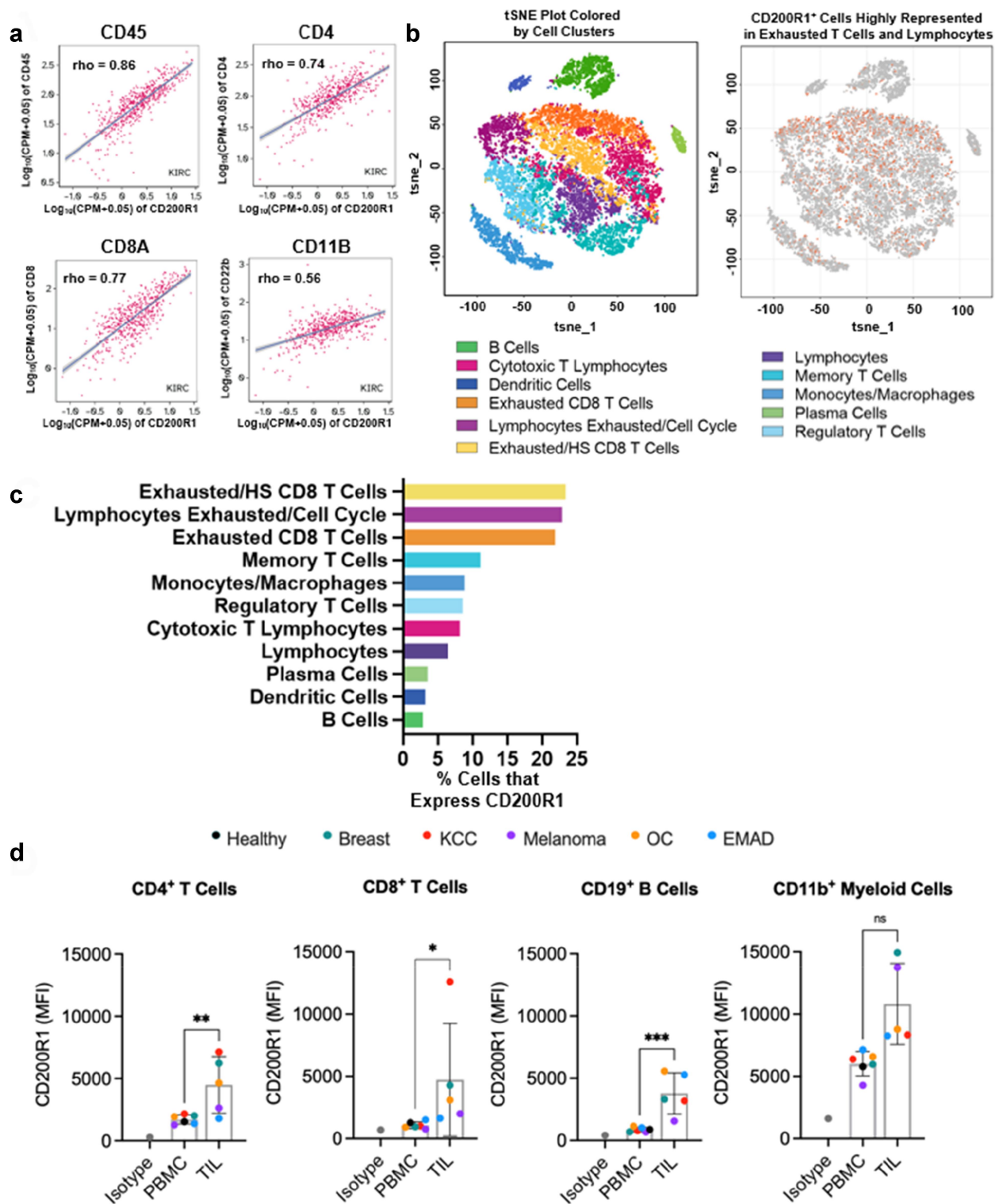


**Figure 2.** CD200R1 is increased on tumor-infiltrating lymphocytes.

a) Expression of *CD200R1* correlates positively with expression of immune-cell markers *CD45*, *CD4*, *CD8*, and *CD11B* in renal clear cell carcinoma; b) Expression of *CD200R1* is enriched in exhausted TIL cell types from melanoma patients previously treated with anti-CTLA4 and anti-PD-1 checkpoint inhibitors (right panel, orange data points); c) Plot of percent of cells that express *CD200R1* in all samples. d) CD200R1 expression on TILs from different tumor types (Breast, Kidney Clear Cell [KCC], Melanoma, Ovarian [OC], and Endometrial Adenocarcinoma [EMAD]) was compared to matched PBMCs from the same patient. A ratio paired t-test was used to determine statistical significance. \*  $p < 0.05$ , \*\*  $p < 0.01$ , \*\*\*  $p < 0.001$ . Healthy PBMCs from 1 donor were also profiled (black dot) as a reference. Fluorescent background was recorded with an isotype-matched control (gray dot).

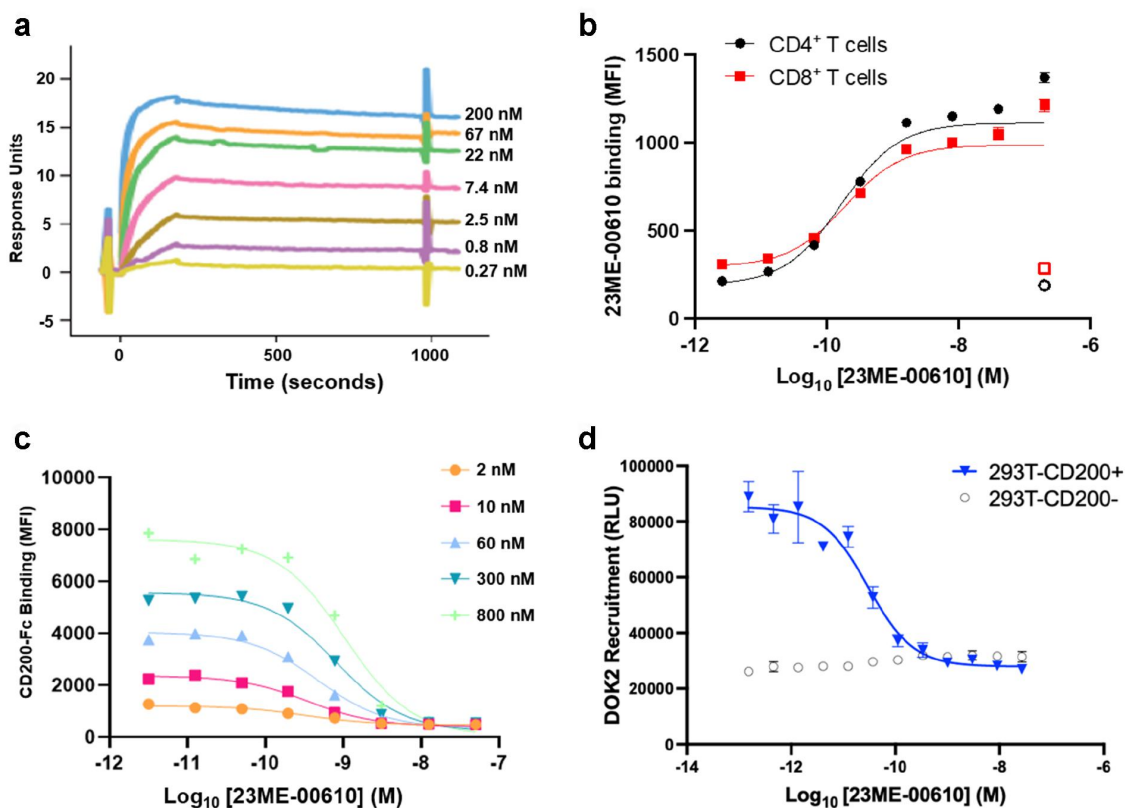


**Figure 3.** 23ME-00610 potently binds CD200R1, blocks CD200 binding, and inhibits downstream signaling.

a) Binding of 23ME-00610 to immobilized human CD200R1 on a CAP chip was evaluated by SPR. A representative sensorgram is shown from 1 of 3 independent experiments using a representative isoform of human CD200R1 (CD200R1-iso4-Alt); b) Donor PBMCs were incubated with serial dilutions of biotinylated 23ME-00610 or 200 nM of biotinylated isotype-matched control (open symbols). Serial dilutions were analyzed by flow cytometry in biological replicates. The median MFI  $\pm$  SD are graphed. c) U937 cells engineered to express CD200R1 were pre-incubated with varying concentrations of biotinylated CD200-Fc (2 to 800 nM) followed by incubation with serial dilutions of 23ME-00610 at 4°C for 30 minutes. MFI values of streptavidin detection are depicted from 1 of 3 independent experiments; d) Jurkat cells were engineered to express CD200R1 and DOK2, each modified at the C-terminus with a separate  $\beta$ -galactosidase enzyme fragment. When co-cultured with HEK293T cells expressing CD200, this reporter cell line induced a chemiluminescent signal reflective of CD200R1 signaling. Serial dilutions of 23ME-00610 were added to the co-culture to evaluate blocking of CD200-induced recruitment of DOK2 to CD200R1. HEK293T cells with no CD200 endogenous expression were used to determine the baseline of signal. Luminescent values from 1 of 6 independent experiments are shown as mean  $\pm$  SD (N=3 replicates for each concentration).

displaced pre-bound ligand with an  $EC_{50}$  ranging from 0.32 to 1.04 nM (Figure 3C).

To measure the capacity of 23ME-00610 to inhibit immunosuppressive intracellular signaling downstream of CD200R1, we evaluated recruitment of the adaptor protein DOK2 to the cytoplasmic tail of CD200R1 in a split-galactosidase-based reporter assay. To induce DOK2 recruitment, CD200R1-expressing Jurkat reporter cells were co-incubated with HEK293T cells engineered to express human CD200. In this reporter-based overexpression system, 23ME-00610 inhibited CD200:CD200R1-mediated recruitment of DOK2 with a mean  $\pm$  SD  $IC_{50}$  value of  $0.02 \pm 0.01$  nM ( $n = 6$ ) (Figure 3D). Together, these data suggest that 23ME-00610 is a potent anti-CD200R1 antibody that can displace CD200 ligand already bound to the receptor, relieving downstream signaling.

We next sought to characterize the capacity of 23ME-00610 to block CD200-mediated suppression of primary T cells. Specifically, human  $CD3^+$  T cells were chronically stimulated with phytohemagglutinin (PHA) and IL-2 for 7 days, then primed with IL-4 for 24 h to mimic the immunosuppressive TME in cancer patients<sup>12</sup> and increase CD200R1 expression<sup>13</sup>, rendering cells more sensitive to CD200-mediated inhibition.

Phenotypic characterization of these chronically stimulated T cells confirmed CD200R1 and PD-1 expression on all four donors (Supplemental Figure S6 and Figure S7). Incubation for 24 h with recombinant CD200-Fc suppressed IL-2 production by an average of  $54 \pm 13\%$ , whereas treatment with 50 nM 23ME-00610 completely rescued CD200-suppressed IL-2 production in all 4 donors tested (Figure 4A). Similar results were obtained when IFN $\gamma$  secretion was analyzed at the same 24h time point with these four donors (Supplemental Figure S8). In an experiment with a 5<sup>th</sup> donor, chronically stimulated T cells were treated for 72 h, a more optimal time point for detecting maximal IFN $\gamma$  levels. 23ME-00610 rescued the CD200-mediated suppression of IFN $\gamma$  secretion with a mean  $\pm$  SD  $EC_{50}$  of  $0.055 \pm 0.014$  nM ( $n = 3$  independent experiments, 5<sup>th</sup> donor) (Figure 4B).

To measure the capacity of 23ME-00610 to reverse immunosuppression in a disease-relevant context, IFN $\gamma$  secretion from staphylococcal enterotoxin B (SEB)-stimulated PBMCs isolated from nine different human cancer patients was measured (Figure 5). SEB was used as a stimulus to polyclonally activate T cells similar to experiments performed to characterize immune checkpoint inhibitors, such as anti-PD-1 and anti-

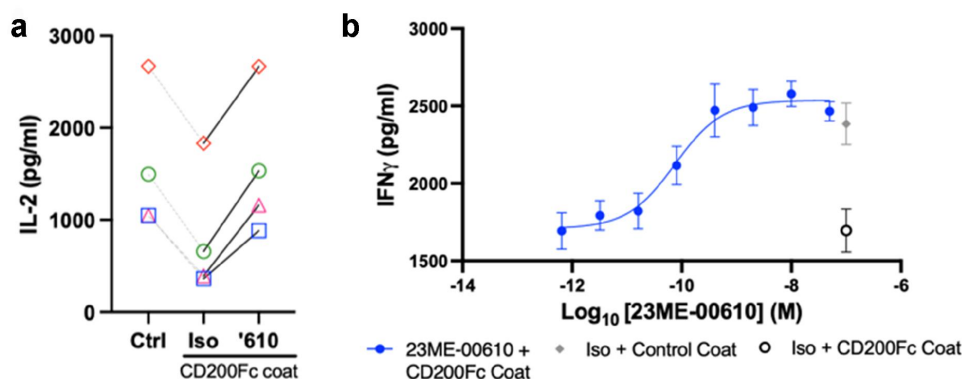


**Figure 4.** 23ME-00610 rescues the immunosuppressive activity of CD200 in T cells.

a) Human pan-T cells isolated from 4 healthy donors were chronically stimulated with phytohemagglutinin and IL-2 for 7 days. Cells were harvested, rested of stimulants, and primed with human IL-4 for 24 hours. Cells were treated with 50 nM isotype control (Iso) or 23ME-00610 ('610) in plates coated with anti-CD3 and CD200-Fc or anti-lysozyme-matched Fc control (Control Coat, Ctrl) for 24 hours. Mean IL-2 secretion levels were graphed for each donor (diamond, circle, square and triangle); b) Cells were stimulated as before, but IFN $\gamma$  levels were measured 72 hours post-treatment with 50 nM isotype control (Iso) or 23ME-00610 in plates coated with anti-CD3 and CD200-Fc or anti-lysozyme-matched Fc control. A representative dose-response curve for 23ME-00610 rescue of IFN $\gamma$  secretion is plotted for the mean of technical quadruplicate measurements  $\pm$  SEM.

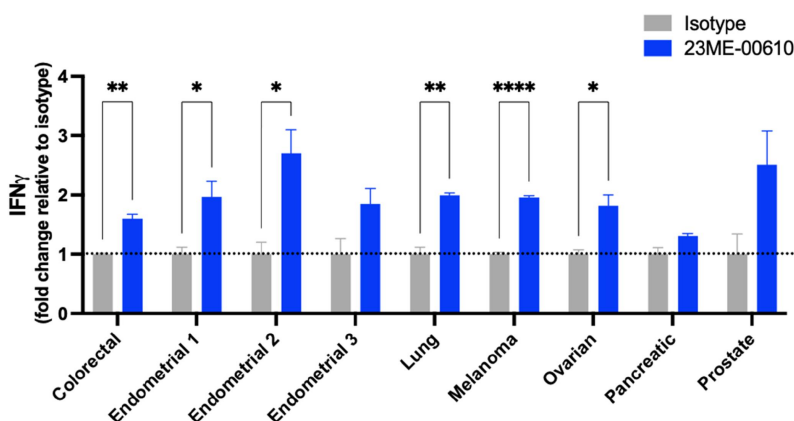


**Figure 5.** 23ME-00610 enhances IFN $\gamma$  secretion from cancer patient PBMCs.

PBMCs from 9 cancer patients were incubated with 100 nM of 23ME-00610 or isotype control. Cells were stimulated with SEB. IFN $\gamma$  levels were determined by ELISA. Mean biologic triplicates were normalized to isotype control. The unpaired t-test was applied to determine statistical significance between 23ME-00610 and Isotype control treatment groups. \*  $p < 0.05$ , \*\*  $p < 0.005$ , \*\*\*\*  $p < 0.00005$ . Each donor was tested once. Data are presented as mean  $\pm$  standard error.

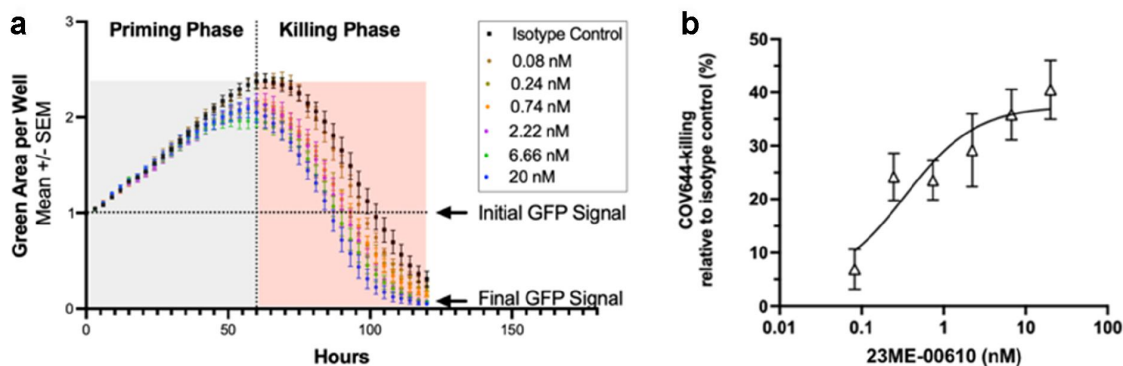


**Figure 6.** 23ME-00610 Enhances PBMC-Mediated Tumor-Cell Killing.

Killing of a tumor cell line that endogenously expresses CD200, COV-644-GFP, by PBMCs was evaluated upon treatment with 23ME-00610 or isotype control. a) CD200R1 + PBMCs were primed with SEB and treated with a titration of 23ME-00610. COV644-GFP cells were co-cultured with PBMCs for 120 hours and GFP signal was monitored as a readout of tumor-cell number. Tumor-cell killing was observed as a decrease in total GFP signal at the end of the experiment relative to the GFP signal observed at the beginning of the experiment. The change in GFP signal over time relative to isotype, in the killing phase, was used to calculate the EC50. b) A representative dose-response curve of tumor-cell killing relative to isotype control; data are represented as the mean  $\pm$  standard error (N = 4 replicates for each concentration) using PBMCs from one donor.

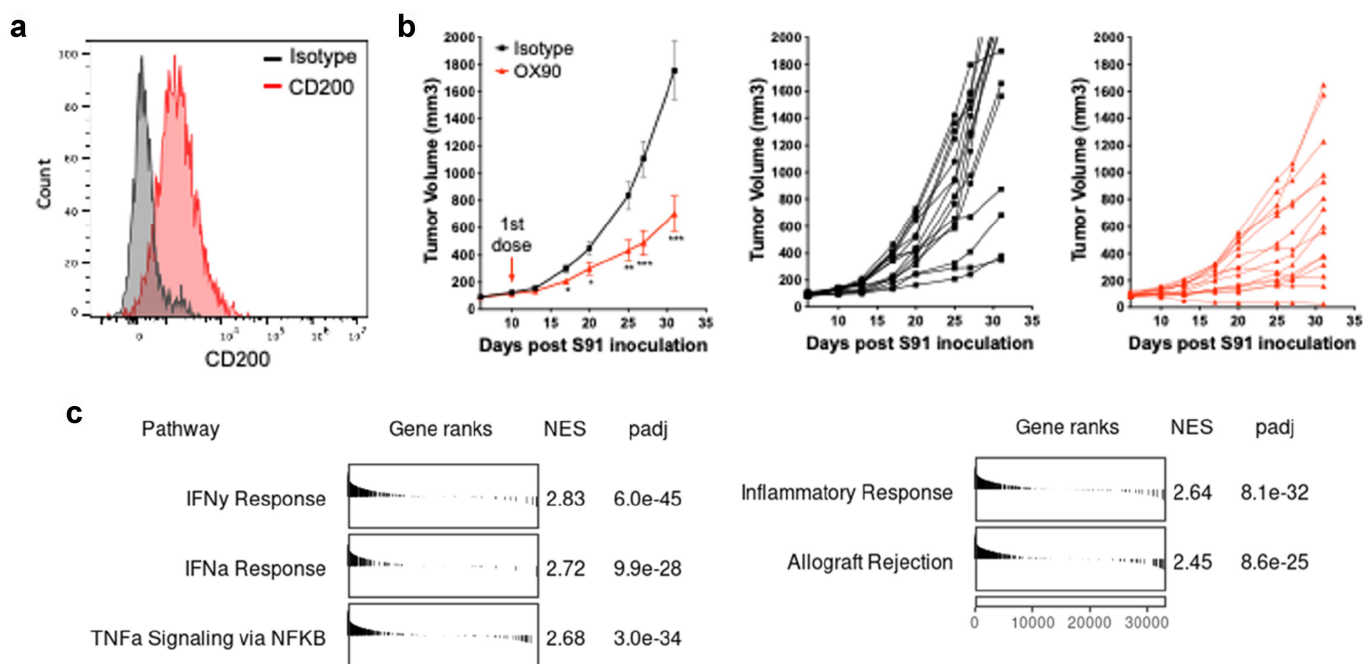


**Figure 7.** Inhibition of the CD200:CD200R1 immune checkpoint elicits an antitumor response in the S91 melanoma mouse model.

a) CD200 cell-surface staining in S91 tumors were analyzed by flow cytometry (Black, Isotype control; Red, CD200). b) S91 cancer cells were subcutaneously injected into DBA/2 mice and were treated when tumor volume reached 100 mm<sup>3</sup> with 20 mg/kg of anti-CD200 (OX90) or Isotype control antibodies twice weekly (n=15/group). Plots shown are mean tumor volume  $\pm$  SEM (left), and individual animal tumor measurements (middle - isotype treated mice, right - OX90-treated mice). Analysis of variance (ANOVA) was used to establish statistical significance; \*  $p < 0.05$ ; \*\*  $p < 0.01$ ; \*\*\*  $p \leq 0.001$ . c) Pathway enrichment analysis of DEGs indicated immune system activation in OX90 treated samples. Enrichment of immune-related pathways are shown with normalized enrichment score (NES) and adjusted p-values.

CTLA-4<sup>14,15</sup>. 23ME-00610 significantly enhanced IFN $\gamma$  secretion from SEB-stimulated PBMCs relative to isotype control in 6 of 9 cancer patient samples tested ( $p < 0.05$ ).

To determine whether 23ME-00610 could activate TILs and induce tumor-cell killing in a system that mimics the immunosuppressive TME, we established a real-time fluorescence-based assay to evaluate tumor cell number. The COV-644 ovarian carcinoma tumor cell line, which expresses CD200 ligand endogenously (Supplemental Figure S9), was engineered to constitutively express green fluorescent protein (GFP). These tumor cells were co-cultured with human PBMCs, which express CD200R1, and the GFP signal was monitored in real time as a fluorescent readout of tumor cell number. As intended, PBMCs became activated and killed the COV-644-GFP tumor cells (termed the “killing phase”) following a variable lag time (termed the “priming phase”) in the presence of isotype control (Figure 6A). In a dose-dependent manner, 23ME-00610 significantly enhanced PBMC-mediated tumor cell killing, with a mean EC<sub>50</sub> of  $2.09 \pm 1.53$  nM ( $n = 3$ ) using PBMCs isolated from one representative donor (Figure 6B).

### CD200:CD200R1 blockade in an in vivo syngeneic mouse model

To evaluate the capacity of antibodies blocking the CD200:CD200R1 immune checkpoint to reinvigorate the immune system and disrupt tumor growth in vivo, we employed

a mouse model of melanoma using the S91 tumor cell line, which expresses high levels of CD200 RNA relative to other cell lines<sup>16</sup>. Expression of CD200 on these tumors was confirmed by flow cytometry (Figure 7A). To block the CD200:CD200R1 signaling pathway, we used an antibody against mouse CD200 (based on the established anti-mCD200 antibody OX90), as 23ME-00610 does not bind mouse CD200R1 and no commercial equivalent was available (Supplemental Table S4). We used a commercial, Fc-silent version of OX90 that lacks the ability to activate antibody-dependent cellular cytotoxicity (ADCC), complement-dependent cytotoxicity (CDC), or phagocytosis, similar to 23ME-00610. Treatment of animals with Fc-silent OX90 resulted in significant tumor growth inhibition (approximately 60% decrease in tumor volume at 32 days after implantation;  $p < 0.001$ ), demonstrating that blockade of CD200:CD200R1 signaling is sufficient for tumor growth inhibition in mice (Figure 7B).

To better understand the mechanism of antitumor activity of in vivo blockade of CD200:CD200R1 signaling, we performed RNA-seq on bulk tumors and analyzed the differences in gene expression between isotype control- and OX90-treated tumors. Pathway enrichment analysis of differentially expressed genes (DEGs) indicated immune system modulation by CD200:CD200R1 blockade. Relevant gene sets that were enriched, such as IFN $\gamma$  and TNF $\alpha$  responses, indicate that CD200:CD200R1 blockade may result in immune and T cell activation in a complex tumor immune environment (Figure 7C).

## Discussion

ICIs have continued to demonstrate durable responses and improved survival across different cancer types in the locally advanced and metastatic setting. The use of ICIs has recently expanded to include early-stage cancers, with compelling outcomes observed in the preoperative setting prior to tumor resection in non-small cell lung cancer (NSCLC), triple negative breast cancer, and MSI-H CRC<sup>17–19</sup>. Despite these advances, the majority of cancer patients experience primary or acquired resistance to current ICI therapies<sup>20</sup>. Discovery and activation of novel immune checkpoints may lead to new therapies for cancers that are inadequately addressed by current therapies.

Human genetics can better inform drug discovery, as drug targets with genetic support have higher success rates in clinical development<sup>21,22</sup>. Additionally, GWAS studies with small sample sizes have demonstrated that germline genetics influence the immune composition of the TME<sup>23</sup>. The 23andMe genetic and health database contains approximately 13.4 million individuals, >80% of whom consent to participate in research. This database enables the study of aggregate, de-identified genetics of millions of participants, alongside more than 4 billion health survey answers. We hypothesized that by analyzing the large-scale 23andMe genetic and health database for genetic variants with pleiotropic, opposing effects in cancer and immune diseases, we could pinpoint areas of the genome that may encode promising I/O targets for therapeutic intervention. Detection of a variant mapping to the known ICI and immuno-oncology target CTLA4 that was associated with opposing effects on autoimmune and inflammatory diseases and cancer confirmed the utility of this approach. Monitoring our genetic and health survey database for a similar pleiotropic signature, we identified three genomic loci with opposing effects in cancers and immune diseases, which mapped to the immune checkpoint proteins CD200, CD200R1, and DOK2.

Clinical data reported for an anti-CD200 antibody, samalizumab, suggest that this antibody was unable to attain concentrations sufficient to fully saturate CD200 on B cells in patients with CD200-expressing B-cell malignancies, potentially limiting its efficacy<sup>24</sup>. As expression of the receptor CD200R1 is predominantly limited to immune cells, an antibody that inhibits CD200:CD200R1 signaling by blocking CD200R1 has the potential to address the limitations of CD200-directed antibodies. To address this, we developed 23ME-00610, a humanized anti-CD200R1 IgG1 mAb, to investigate the impact of CD200R1 blockade on antitumor immune response.

Immune-cell “exhaustion” is a phenotypic hallmark of TILs in chronic diseases, including cancer, in which immune cells are chronically exposed to activation and immunosuppressive signals from the microenvironment. Such exhausted TILs exhibit altered immune function, including impaired effector function, upregulated regulatory or inhibitory receptors, and a consequential decrease in antitumor activity. Therefore, agents that can reverse immune-cell exhaustion or “rescue” the immunosuppressive tumor microenvironment that contributes to the exhausted state have the potential to reactivate antitumor immune responses. In cancer patients who had previously been treated with ICI therapies, we observed that CD200R1 was most highly expressed in exhausted lymphocyte groups,

which were differentially expanded in ICI nonresponders. This expression pattern suggests that ICI nonresponder tumors may be evading checkpoint inhibition via the CD200:CD200R1 signaling axis and may benefit from therapeutic antibodies targeting CD200R1. Therefore, we performed experiments with chronically stimulated T-cells and demonstrated that 23ME-00610 was able to potently and effectively rescue CD200-mediated suppression of T cell secretion of IL-2 and IFN $\gamma$ . 23ME-00610 was also able to enhance the effector functions of cancer patient PBMCs and PBMCs from healthy donors cocultured with CD200-expressing tumor cells. Since the T cell-stimulating agent SEB was used in experiments with PBMCs and we have observed that SEB stimulation of PBMCs results in expansion of T cells relative to other cell types, it is likely, though not conclusive that T cells are the responsible cell type for 23ME-00610 mechanism of action in experiments with PBMCs.

Humans express a single functional CD200R1 inhibitory gene, whereas mice express multiple CD200 family receptors that act as both stimulatory and inhibitory molecules<sup>2</sup>. Differences in the pathway between mice and humans may confound interpretation of data relative to human systems, especially when considering agents that modulate CD200R1 activity. Despite these limitations, modeling of the complex TME is best recapitulated in syngeneic mouse models, so we investigated the blockade of CD200:CD200R1 signaling in mice bearing murine S91 melanoma tumors that endogenously express CD200. OX90, a CD200 blocking antibody clone that has been frequently used in published studies, was originally isolated in a rat IgG2a backbone<sup>25</sup>. Rat IgG2a can bind weakly to mouse Fc $\gamma$ RIII and may mediate depletion of CD200 positive cells<sup>26</sup>. This could result in confounding effects as CD200 is broadly expressed, including on S91 tumor cells, B cells, and activated T cells. To avoid this, we used an Fc-silent version of OX90 for our studies, which should limit pharmacological effects to blocking CD200:CD200R1 signaling. We observed that blocking CD200:CD200R1 signaling was sufficient to promote significant tumor growth inhibition and activate expression of genes involved in immune activation, such as the IFN $\gamma$  and TNF $\alpha$  pathways, which have been shown to be critical for CTL-mediated killing of cancer cells<sup>27,28</sup>.

In summary, we have used germline genetic data to prioritize therapeutic targets for immune modulatory oncology therapeutics. 23ME-00610, a first-in-class anti-CD200R1 antibody, is being evaluated in a first-in-human (FIH) Phase 1/2 trial in patients with advanced solid malignancies to assess its safety, tolerability, pharmacokinetic profile, and preliminary anticancer activity (NCT05199272).

## Acknowledgments

Scientific writing and editorial assistance was provided by Rand Miller, Ph.D. We would like to thank Steve Pitts, Adam Auton, Alex Owyang, Germaine Fuh, and Louise Scharf for their scientific guidance. We thank past and present 23andMe Therapeutics scientists who contributed to 23ME-00610, including Ben Chung, Pete Yeung, Patrick Koenig, Lance Larrabee, Jean Crilly, Mike Eby, Tina Thai, Shiteng Duan, Suk Lee, Dina Ayupova, Sushil Kumar, and Pierre Fontanillas. 23andMe is grateful to the millions of participants who consented to using their genetic and health survey data for research.



The results associated with TCGA are based upon data generated by the TCGA Research Network: <https://www.cancer.gov/tcga>.

## Disclosure statement

XF, YH, CM, ELL, TP, AZ, MP, SRM, DG, MS, CCL: Employees of 23andMe JF, CB, CL, ZY, WC, AC: Employees of 23andMe at the time this work was performed

## Funding

This work was funded by 23andMe.

## Data availability statement

The data that support the findings of this study are available upon reasonable request.

## List of Abbreviations

ADCC	antibody-dependent cellular cytotoxicity
CDC	complement-dependent cytotoxicity
CTLA-4	cytotoxic T-lymphocyte-associated protein 4
DEG	differentially expressed gene
DOK	downstream of tyrosine kinase
EC <sub>50</sub>	half-maximal effective concentration
ELISA	enzyme-linked immunosorbent assay
EMAD	endometrial adenocarcinoma
Fc	fragment crystallizable
FIH	first-in-human
GFP	green fluorescent protein
GWAS	genome-wide association study
I/O	immuno-oncology
ICI	immune checkpoint inhibitor
Ig	immunoglobulin
KCC	kidney clear cell carcinoma
K <sub>D</sub>	equilibrium dissociation constant
mAb	monoclonal antibody
MoDC	monocyte-derived dendritic cell
NSCLC	non-small cell lung cancer
OC	ovarian cancer
PBMC	peripheral blood mononuclear cell
PCA	principle component analysis
PD-1	programmed cell death protein 1
RasGAP	Ras GTPase activating protein
SD	standard deviation
TCGA	The Cancer Genome Atlas
TIL	tumor-infiltrating lymphocyte
TME	tumor microenvironment

## References

- Schoenfeld AJ, Hellmann MD. Acquired resistance to immune checkpoint inhibitors. *Cancer Cell*. 2020;37(4):443–455. doi:10.1016/j.ccell.2020.03.017.
- Wright GJ, Cherwinski H, Foster-Cuevas M, Brooke G, Puklavec MJ, Bigler M, Song Y, Jenmalm M, Gorman D, McClanahan T, et al. Characterization of the CD200 receptor family in mice and humans and their interactions with CD200. *J Immunol*. 2003;171(6):3034–3046. doi:10.4049/jimmunol.171.6.3034.
- Rijkers ES, de Ruiter T, Baridi A, Veninga H, Hoek RM, Meyaard L. The inhibitory CD200R is differentially expressed on human and mouse T and B lymphocytes. *Mol Immunol*. 2008;45(4):1126–1135. doi:10.1016/j.molimm.2007.07.013.
- Rygiel TP, Meyaard L. CD200R signaling in tumor tolerance and inflammation: a tricky balance. *Curr Opin Immunol*. 2012;24(2):233–238. doi:10.1016/j.coi.2012.01.002.
- Mihrshahi R, Barclay AN, Brown MH. Essential roles for Dok2 and RasGAP in CD200 receptor-mediated regulation of human myeloid cells. *J Immunol*. 2009;183(8):4879–4886. doi:10.4049/jimmunol.0901531.
- Zhang S, Cherwinski H, Sedgwick JD, Phillips JH. Molecular mechanisms of CD200 inhibition of mast cell activation. *J Immunol*. 2004;173(11):6786–6793. doi:10.4049/jimmunol.173.11.6786.
- Misstear K, Chanas SA, Rezaee SAR, Colman R, Quinn LL, Long HM, Goodyear O, Lord JM, Hislop AD, Blackbourn DJ. Suppression of antigen-specific T cell responses by the Kaposi's sarcoma-associated herpesvirus viral OX2 protein and its cellular orthologue, CD200. *J Virol*. 2012;86(11):6246–6257. doi:10.1128/JVI.07168-11.
- Herbrich S, Baran N, Cai T, Weng C, Aitken MJL, Post SM, Henderson J, Shi C, Havranek O, Richard-Carpentier G, et al. Overexpression of CD200 is a stem cell-specific mechanism of immune evasion in AML. *J Immunother Cancer*. 2021;9(7):e002968. doi:10.1136/jitc-2021-002968.
- Shafiei-Jahani P, Helou DG, Hurrell BP, Howard E, Quach C, Painter JD, Galle-Treger L, Li M, Loh YHE, Akbari O. CD200–CD200R immune checkpoint engagement regulates ILC2 effector function and ameliorates lung inflammation in asthma. *Nat Commun*. 2021;12(1):2526. doi:10.1038/s41467-021-22832-7.
- Heilbron K, Mozaffari SV, Vacic V, Yue P, Wang W, Shi J, Jubbs AM, Pitts SJ, Wang X. Advancing drug discovery using the power of the human genome. *J Pathol*. 2021;254(4):418–429. doi:10.1002/path.5664.
- Sade-Feldman M, Yizhak K, Bjorgaard SL, Ray JP, de Boer CG, Jenkins RW, Lieb DJ, Chen JH, Frederick DT, Barzily-Rokni M, et al. Defining T cell states associated with response to checkpoint immunotherapy in Melanoma. *Cell*. 2018;175(4):998–1013 e20. doi:10.1016/j.cell.2018.10.038.
- Goldstein R, Hanley C, Morris J, Cahill D, Chandra A, Harper P, Chowdhury S, Maher J, Burbridge S. Clinical investigation of the role of interleukin-4 and interleukin-13 in the evolution of prostate cancer. *Cancers (Basel)*. 2011;3(4):4281–4293. doi:10.3390/cancers3044281.
- Blom LH, Martel BC, Larsen LF, Hansen CV, Christensen MP, Juel-Berg N, Litman T, Poulsen LK. The immunoglobulin superfamily member CD200R identifies cells involved in type 2 immune responses. *Allergy*. 2017;72(7):1081–1090. doi:10.1111/all.13129.
- Wang C, Thudium KB, Han M, Wang X-T, Huang H, Feingersh D, Garcia C, Wu Y, Kuhne M, Srinivasan M, et al. In vitro characterization of the anti-PD-1 antibody nivolumab, BMS-936558, and in vivo toxicology in non-human primates. *Cancer Immunol Res*. 2014;2(9):846–856. doi:10.1158/2326-6066.CIR-14-0040.
- Selby MJ, Engelhardt JJ, Johnston RJ, Lu L-S, Han M, Thudium K, Yao D, Quigley M, Valle J, Wang C, et al. Preclinical development of ipilimumab and nivolumab combination immunotherapy: mouse tumor models, in vitro functional studies, and cynomolgus macaque toxicology. *PLoS One*. 2016;11(9):e0161779. doi:10.1371/journal.pone.0161779.
- Crown\_Bioscience. MuBase. 2022.
- Keytruda (pembrolizumab). *Prescribing information*. Merck. 2022 [cited 2022; Available from: [https://www.merck.com/product/usa/pi\\_circulars/k/keytruda/keytruda\\_pi.pdf](https://www.merck.com/product/usa/pi_circulars/k/keytruda/keytruda_pi.pdf)].
- Opdivo (nivolumab). *Prescribing information*. Bristol-Myers Squibb. 2022 [cited 2022; Available from: [https://packageinserts.bms.com/pi/pi\\_opdivo.pdf](https://packageinserts.bms.com/pi/pi_opdivo.pdf)].
- Yervoy (ipilimumab). *Prescribing information*. Bristol-Myers Squibb. 2022 [cited 2022; Available from: [https://packageinserts.bms.com/pi/pi\\_yervoy.pdf](https://packageinserts.bms.com/pi/pi_yervoy.pdf)].
- Jenkins RW, Barbie DA, Flaherty KT. Mechanisms of resistance to immune checkpoint inhibitors. *Br J Cancer*. 2018;118(1):9–16. doi:10.1038/bjc.2017.434.

21. Nelson MR, Tipney H, Painter JL, Shen J, Nicoletti P, Shen Y, Floratos A, Sham PC, Li MJ, Wang J, et al. The support of human genetic evidence for approved drug indications. *Nat Genet.* 2015;47(8):856–860. doi:10.1038/ng.3314.
22. Ochoa D, Karim M, Ghoussaini, Hulcoop DG, McDonagh EM, Dunham I. Human genetics evidence supports two-thirds of the 2021 FDA-approved drugs. *Nat Rev Drug Discov.* 2022;21(8):551. doi:10.1038/d41573-022-00120-3.
23. Sayaman RW, Saad M, Thorsson V, Hu D, Hendrickx W, Roelands J, Porta-Pardo E, Mokrab Y, Farshidfar F, Kirchhoff T, et al. Germline genetic contribution to the immune landscape of cancer. *Immunity.* 2021;54(2):367–386 e8. doi:10.1016/j.immuni.2021.01.011.
24. Mahadevan D, Lanasa MC, Farber C, Pandey M, Whelden M, Faas SJ, Ulery T, Kukreja A, Li L, Bedrosian CL, et al. Phase I study of samalizumab in chronic lymphocytic leukemia and multiple myeloma: blockade of the immune checkpoint CD200. *J ImmunoTher Cancer.* 2019;7(1):227. doi:10.1186/s40425-019-0710-1.
25. Hoek RM, Ruuls SR, Murphy CA, Wright GJ, Goddard R, Zurawski SM, Blom B, Homola ME, Streit WJ, Brown MH, et al. Down-regulation of the macrophage lineage through interaction with OX2 (CD200). *Science.* 2000;290(5497):1768–1771. doi:10.1126/science.290.5497.1768.
26. Wang X, Zha H, Wu W, Yuan T, Xie S, Jin Z, Long H, Yang F, Wang Z, Zhang A, Gao J. CD200(+) cytotoxic T lymphocytes in the tumor microenvironment are crucial for efficacious anti-PD-1/PD-L1 therapy. *Sci Transl Med.* 2023. 15(679): p. eabn5029.
27. Kearney CJ, Vervoort SJ, Hogg SJ, Ramsbottom KM, Freeman AJ, Lalaoui N, Pijpers L, Michie J, Brown KK, Knight DA, et al. Tumor immune evasion arises through loss of TNF sensitivity. *Sci Immunol.* 2018;3(23):3(23). doi:10.1126/sciimmunol.aar3451.
28. Dunn GP, Koebel CM, Schreiber RD. Interferons, immunity and cancer immunoediting. *Nat Rev Immunol.* 2006;6(11):836–848. doi:10.1038/nri1961.